

# Novel Multiband Millimeter Wave Antennas

Abdullah Khan Galib<sup>1</sup>, Nayan Sarker<sup>2\*</sup>, and M. Rubaiyat Hossain Mondal<sup>1</sup>

<sup>1</sup>Institute of Information and Communication Technology (IICT), Bangladesh University of Engineering and Technology (BUET), Dhaka-1000, Bangladesh

<sup>2</sup>Department of Electrical and Electronic Engineering (EEE), Jatiya Kabi Kazi Nazrul Islam University, Mymensingh-2220, Bangladesh

Email: galib.eee2010@gmail.com; rubaiyat97@yahoo.com

**Abstract**—The design of multiband antennas is useful for providing multiple resonance frequencies required for multiple application scenarios. However, there is a scarcity of compact-sized antennas in the 70-110 GHz band. In this regard, this paper proposes two multiband millimeter wave antennas in the W and D bands. A small-sized antenna operating at five different frequencies (penta band) with an overall dimension of  $4.8 \times 5.4 \text{ mm}^2$  and resonances at 35.84 GHz, 46.07 GHz, 56.74 GHz, 81.6 GHz, and 110.09 GHz is proposed first. The second one is an array antenna from the first antenna with a size of  $11.1 \text{ by } 6.4 \text{ mm}^2$  and resonances at 28.03 GHz, 36.5 GHz, 53.11 GHz, 65.98 GHz, 77.64 GHz, 89.3 GHz, 100.52 GHz, 111.74 GHz, and 122.19 GHz. Computer Simulation Technology (CST) Microwave Studio tool is used for antenna design purposes. At the two larger frequencies of 81.6 GHz and 110.09 GHz of the first antenna, (the BW, the directivity, the gain, and radiation efficiency) are (3.3 GHz, 6.486 dBi, 6.22 dB, and 94.06%), and (10.01 GHz, 8.797 dBi, 8.506 dB, and 93.52%), respectively. At 77.64 GHz, and 111.74 GHz of the array antenna, (the BW, the directivity, the gain, and radiation efficiency) are (3.73 GHz, 12.35 dBi, 10.68 dB, and 67.9%), (4.4 GHz, 15.31 dBi, 14.07 dB, and 75.23%), respectively. The advantage of the proposed antennas over the currently available 80 GHz and 110 GHz antennas is that they are compact in size while maintaining high bandwidth and gain. Hence, the proposed antennas have potential applications in satellite communications, the Internet of things, compact biomedical devices, and interferometry radars.

**Index Terms**—Array antenna, millimeter wave, resonance, W-Band, D-Band, bandwidth

## I. INTRODUCTION

The millimetre-wave band (mm-wave) (30 to 300) GHz is an interesting subject for researchers due to its exceptional transmission capability through environmental obstacles [1]. The ever-increasing demand for high-speed point-to-point wireless communication has reached a new high. It is time to improve the current communication system's speed because at lower carrier frequencies bandwidth became very congested. As a result, it is a very challenging task to modulate the signal at lower frequency bands with higher-order modulation techniques. Eying at the requirement of the future networks, larger communication bandwidth is a prerequisite in both outdoor long-distance and indoor

small distance point-to-point wireless communication. It is time to gradually shift towards the higher millimetre wave carrier frequencies [2]. The W band is a portion of the mm-wave that starts from 75 GHz and ends at 110 GHz [1]-[4]. The frequencies which are above the W band are termed as D band starting from 110 GHz to 170 GHz which is also part of the Terahertz region (0.1 THz to 10 THz) [5]-[8]. The W band opens up a new brunch of application areas such as high-speed data communications both video and audio, radar communication, detecting weapons as well as biomedical imaging applications. Millimeter-wave has the advantage of reflection and refraction so it can penetrate through buildings, trees, mountains, etc., thus signals can be transmitted easily for dozens of kilometers [3].

Terahertz (THz) region is a comparatively new section of electromagnetic (em) band, but it created a lot of interest among scholars because of its vast application areas. This terahertz band is suitable in many sectors, for example, satellite and radar communications, biomedical applications, astronomy, encryption and so on [9]. In the THz region, there is a high requirement for an effective antenna that will be a low loss, large bandwidth and smaller in dimension. In the THz region, the expectation is high-capacity wireless communication with wide bandwidth [9]-[10]. The W band has several exciting commercial applications like automotive radar at 77 GHz [3]-[4]. Outdoor 10 Gbps networks at 71-76 GHz and 81-86 GHz, both this range is also allocated to satellite services [3], also medical and security imaging and military applications at 94 GHz [11]-[14]. In space applications and at high altitude communications, W band delivers high data rate throughput [3].

In the D band for high operating frequencies, there are small wavelengths and large bandwidths available. Due to these reasons, radars offer both small form factors and compact realization and high-resolution range sensing [5]. This band is used in imaging systems for plasma diagnostics [6], and the detection of hidden weapons or plastic explosive packages. It also can be used for applications like remote atmospheric sensing and space research [15].

In the literature [16]-[24], there are not many antennas reported in both W and D bands. However, various countries use various frequency bands for a similar type of wireless communications. On the other hand, multiple

Manuscript received June 30, 2022; revised December 12, 2022; accepted December 26, 2022.

\*Corresponding author email: nayan\_ece09@yahoo.com.

frequencies for multiple applications are used inside a country. So, the design of an antenna having multiple resonance frequencies is suitable for numerous applications [16]. A very limited number of research papers are found in W band and D band antenna design [1]-[5], [14]-[20], [25]-[27]. Of the reported antennas, few are complicated in design, most of them are either single band or array antennas with a larger size. The author in [1] reported a small size antenna with a central frequency of 94 GHz with three different substrates resulting in three different bandwidths and gain: (8 GHz, 2 GHz, 12 GHz) and (8.56dB, 1.99dB, and 6.32dB) respectively. The work in [3] reports a dual-band antenna at (85 and 94) GHz with a gain of 8.28 dB and 8.89 dB and bandwidth of 7.25 GHz and 1.7 GHz. Another single band antenna with a frequency at 94 GHz is reported in [4] with a bandwidth around 7 GHz and a gain of 23 dBi. The author in [14] reported an antenna having frequencies at (83 and 94) GHz with a bandwidth of 5.45 GHz and 3.2 GHz respectively and a gain of 8.4 dBi and 8.9 dBi respectively. The author in [17] reported an antenna at a frequency of 85.5 GHz which enables 1.7-km wireless delivery with a data rate of 20-Gb/s. A dual-band antenna with high gain is reported in a study [6]. The maximum gain is 49.6 dB at a frequency of 94.05 GHz and 44.1 dB at a frequency of 35.5 GHz. A tri-band antenna is reported in [19] with frequencies at 86 GHz, 97 GHz, and 104 GHz. The gain on these frequencies is more than 10 dBi. The author of [20] reported an antenna with a frequency of 94 GHz having a bandwidth of 34.3 GHz and a gain of 16.7 dB.

The author in [5] reported an antenna at the D band with a frequency of 160 GHz having a BW of 10 GHz and a gain of 7 dBi with 60 % efficiency. A multilayer layer 6x6 Mushroom Electromagnetic Bandgap (MEBG) antenna with a frequency of 122GHz is reported in [7]. Another antenna at a frequency of 122 GHz is reported in [8] with a bandwidth of 7.6 GHz and a gain of 6.9 dBi. The author of [20] reported an antenna with a frequency at 140 GHz and a 36 % BW of 50.3 GHz with a range from 115.3-165.6 GHz with a gain of 7.4 dBi. The author in [25] reports a single element antenna and an array antenna both with a frequency at 143 GHz with a BW of 20 GHz, both the antennas having a gain of 7 dBi and 14 dBi, respectively. A grid array antenna at a frequency of 146 GHz is reported in [26]. The antenna has a BW of 21 GHz and a gain of 14.5 dBi. The author of [27] reported an antenna with a gain of 4.7 dBi, BW of 14 GHz, and radiation efficiency of 43% at a frequency of 130 GHz.

Two small-sized multiband antennas in the W band and D band are proposed in this work. The objectives of this research work are summarized here. A low dimension penta band mm-wave antenna with operating frequencies around 80 GHz and 110 GHz at the W band is proposed. Then a multiband array antenna is designed based on the proposed single element antenna in the W and D bands. Furthermore, the antenna's overall performances are investigated based on return loss (S-

parameter), bandwidth, radiation patterns, gain, and efficiency [28]-[31].

The remaining parts of this research work are organized as follows. The design procedure in Computer Simulation Technology (Microwave studio) is discussed in Section II. Simulation results of both antennas are presented in Section III. A comparative study of the antennas is provided in Section IV. Finally, in Section V, concluding remarks and the future scope are presented.

## II. DESIGN OF TWO ANTENNAS AT MM BAND

The design procedure of both the proposed antennas is described in this section. To simulate and optimize the proposed antennas Computer Simulation Technology (CST) Microwave Studio tool is used. The design reported in [16] is modified to design the first antenna. In this antenna design FR4 (lossy) substrate with dielectric constant  $\epsilon_r=4.3$ , and dielectric loss,  $\tan \delta = 0.025$  is used.

The substrate thickness is  $h = 1.6$  mm and the thickness of copper metal is  $t = 0.1$  mm. The description of the detailed design procedure is in the next section.

### A. Single Antenna Design

The plan view and perspective 3-D view of the antenna are mentioned in Fig. 1. The performance of the designed antenna is optimized at five distinct frequencies at  $f_{r1,1}=35.84$  GHz,  $f_{r1,2}=46.07$  GHz,  $f_{r1,3}=56.74$  GHz,  $f_{r1,4}=81.6$  GHz, and  $f_{r1,5}=110.09$  GHz. The different yellow-coloured arms of the individual F patterns of the proposed antenna control the overall radiation.

TABLE I: DIMENSIONS OF SINGLE ANTENNA

Antenna parameters	Length in mm
$W_{sub}$	4.8
$L_{sub}$	5.4
$W_1$	2.0
$L_1$	2.0
$W$	0.6
$L$	0.4
$L_2$	0.95
$L_3$	0.8
$W_2$	1.7
$W_3$	1.5
$W_4$	1.9
$W_5$	2.1
$W_6$	2.1
$L_4$	0.45
$G_1$	0.1
$G_2$	0.1
$a = b$	1.0

Different arm length of the antenna is adjusted using the CST optimization tool to enhance the overall performance of the antenna. The penta band antenna's optimized parameters are presented in Table I.

The volume of the antenna is  $4.8 \times 5.4 \times 1.8$  mm<sup>3</sup>. From the Fig. 1 3-D view, it is seen that the antenna has three layers. Two metal layers and one dielectric layer. The metal layer is marked by yellow colour and the dielectric layer is marked by sky blue colour. In the plan view, it is seen that there are two identical square shape elements with a length  $L_1 = 2$  mm and width  $W_1 = 2$  mm at the bottom. Those two squares are separated by  $W = 0.6$  mm. The 10 dB impedance bandwidth and overall bandwidth are controlled by this  $W$ . Inside of those two square portions are cut by two square-shaped slots with a length of  $a = b = 1$  mm. The gap on either side of  $W$  is very

small. Those two gaps are  $G_1 = 0.1$  mm and  $G_2 = 0.1$  mm respectively. Now on the left side, the first F pattern consists of arm  $W_2 = 1.7$  mm and arm  $W_5 = 2.1$  mm, while on the right side the second F pattern is made with  $W_3 = 1.5$  mm and  $W_4 = 1.9$  mm. To get a higher frequency resonance band, the arm  $W_6 = 2.1$  mm at the top of the design is set. By varying the arm length, resonance frequency values can be changed. The resonance frequencies increase when the value of arm  $W_5$  and  $W_6$  decreases but after a specific value, the number of resonance bands decreases from five to four. Using fringing field effect and size optimization techniques available in the CST, the designed antenna size is reduced than the antenna reported in [18], [19]. After the optimization is done in CST, the desired performance of the antenna is achieved.

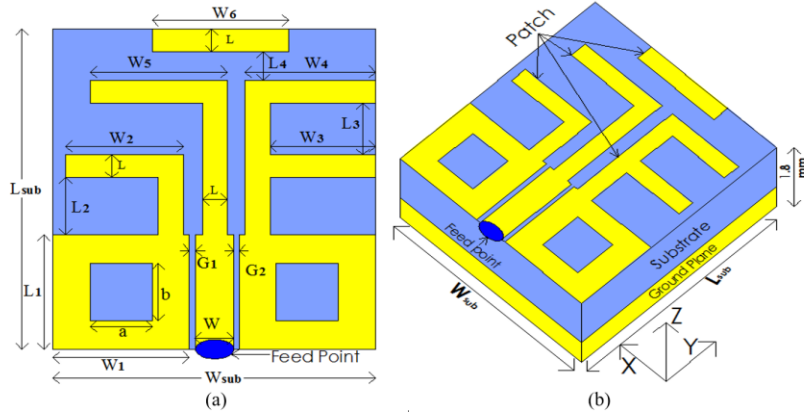


Fig. 1. (a) for 2-D and (b) for 3 D view of the multiband millimetre wave single antenna.

### B. Array Antenna Design

TABLE II: DIMENSIONS OF ARRAY ANTENNA

Antenna parameters	Length in mm
$W_{sub2}$	11.1
$L_{sub2}$	6.4
$W_1 = L_1$	2.0
$W$	0.6
$L$	0.4
$L_2$	0.95
$L_3$	0.8
$W_2$	1.7
$W_3$	1.5
$W_4$	1.9
$W_5 = W_6$	2.1
$W_7$	5.7
$L_4$	0.45
$L_5$	0.2
$G_1 = G_2$	0.1
$G_p$	1.5
$a = b$	1.0

The array is designed from a single antenna to get high gain and directivity. In this antenna design FR4 (lossy) substrate with dielectric constant,  $\epsilon_r = 4.3$ , and dielectric loss,  $\tan \delta = 0.025$  is used. The substrate thickness is  $h = 1.0$  mm and the copper metal thickness is  $t = 0.1$  mm. The 2-D plan view and perspective 3-D view of the antenna are presented in Fig. 2 and Fig. 3. There are two array elements in this array antenna. From the figure, it is seen that the  $W$  of both array element is extended by length  $L$  and those two array element is connected by  $W_7 = 6.9$  mm. The spacing between two array elements is  $G_p = 1.5$  mm. This gap is maintained keeping in mind to avoid mutual coupling and grating lobe which is less than half of the wavelength. The antenna fed is given at  $L_5 = 0.2$  mm which is connected to  $W_7$ . The optimized dimensional parameters of the nona-band antenna are shown in Table II. The optimized antenna performance is evaluated in the resonance frequencies at  $f_{r2,1} = 28.03$  GHz,  $f_{r2,2} = 36.5$  GHz,  $f_{r2,3} = 53.11$  GHz,  $f_{r2,4} = 65.98$  GHz,  $f_{r2,5} = 77.64$  GHz,  $f_{r2,6} = 89.3$  GHz,  $f_{r2,7} = 100.52$  GHz,  $f_{r2,8} = 111.74$  GHz and  $f_{r2,9} = 122.19$  GHz.

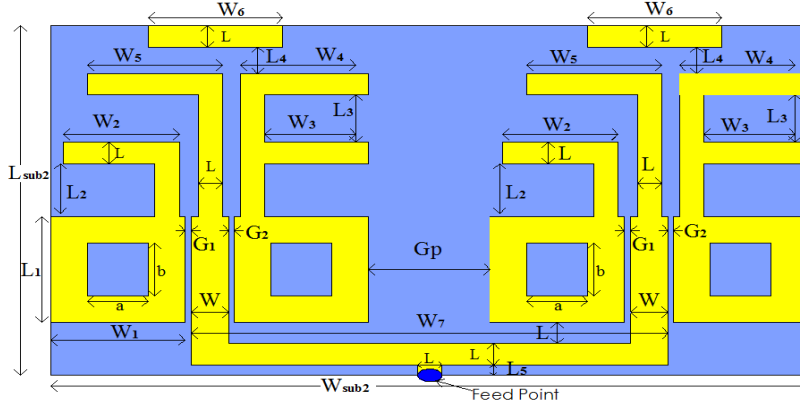


Fig. 2. 2-D view of the multiband millimetre wave array antenna.

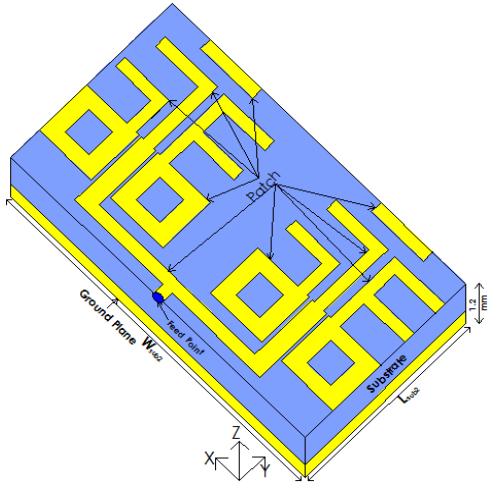


Fig. 3. 3-D view of the multiband millimetre wave array antenna.

### III. SIMULATION RESULTS OF THE ANTENNA PERFORMANCE

This section presents the performance of both the antennas simulated using CST. The antenna performance is evaluated based on return loss (S-Parameter) and BW, radiation patterns, gain, and efficiency.

#### A. Simulation Results of the Single Antenna

The optimized results of the designed antenna using waveguide ports are at resonance frequencies at  $f_{r1,1}=35.84$  GHz,  $f_{r1,2}=46.07$  GHz,  $f_{r1,3}=56.74$  GHz,  $f_{r1,4}=81.6$  GHz, and  $f_{r1,5}=110.09$  GHz are presented in this section.

##### 1) Return loss (s-parameter) and bandwidth

The simulated return loss at  $f_{r1,1}$  is 27.453 dB, at  $f_{r1,2}$  is 15.365 dB, at  $f_{r1,3}$  is 16.858 dB, at  $f_{r1,4}$  is 24.448 dB and at  $f_{r1,5}$  is 15.905 dB, which are mentioned in Fig. 4. All the return losses are less than -10 dB which indicates antenna impedance and the waveguide port impedance is considerably matched. Fig. 4 also shows impedance BW at these five resonances are 4.84 GHz with a span from 33.09 GHz to 37.93 GHz, 3.63 GHz with a span from 43.98 GHz to 47.61 GHz, 2.42 GHz with a span from 55.42 GHz to 57.84 GHz, 3.3 GHz with a span from 79.95 GHz to 83.25 GHz, and 10.01 GHz with a span from 107.12 GHz to 117.13 GHz, respectively. The % BW of the single antenna is 13.5%, 7.87%, 4.26%, 4.04, and 9.09% at  $f_{r1,1}$ ,  $f_{r1,2}$ ,  $f_{r1,3}$ ,  $f_{r1,4}$  and  $f_{r1,5}$ , respectively.

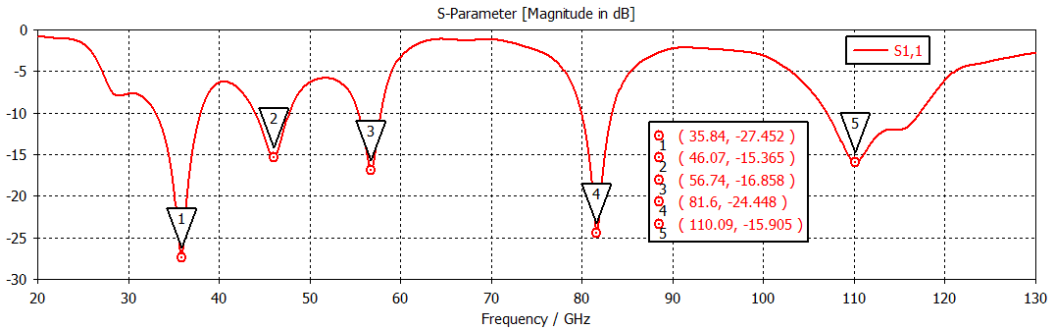


Fig. 4. Reflection co-efficient (S11) of the multiband millimetre wave antenna.

##### 2) Radiation pattern

Fig. 5 to Fig. 9 show far field E and H-field patterns at  $f_{r1,1}$ ,  $f_{r1,2}$ ,  $f_{r1,3}$ ,  $f_{r1,4}$ , and  $f_{r1,5}$ , respectively indicating magnitude the magnitude of main lobe, half power beam width (3 dB) and side lobe magnitude. Fig. 5 shows the far field E and H-field patterns at  $f_{r1,1} = 35.84$  GHz. At

this frequency the magnitude and direction of main lobe, half power beam width (3 dB) and side lobe magnitude are -3.45 dB and 45.00, 250.50, respectively at E- plane. Moreover, the magnitude and direction of main lobe, half power beam width (3 dB) and side lobe magnitude are 5.46 dB and 89.00, 89.30, -5.1 dB, respectively at H- plane.

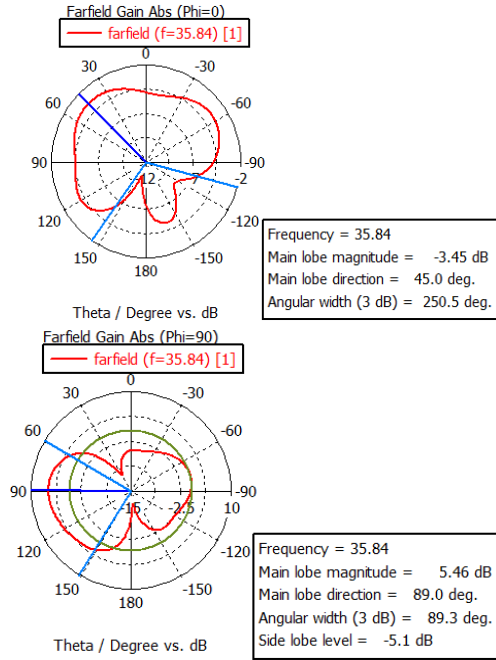


Fig. 5. E and H-plane radiation patterns for multiband millimetre antenna at  $f_{r1,1} = 35.84$  GHz.

Fig. 6 shows the radiation pattern of electric field and magnetic field at  $f_{r1,2} = 46.07$  GHz. At this frequency the magnitude and direction of main lobe, half power beam width (3 dB) and side lobe magnitude are -2.62 dB and 25.00, 57.90, -1.2 dB, respectively at E- plane. Moreover, the magnitude and direction of main lobe, half power beam width (3 dB) and side lobe magnitude 6.22 dB and 44.00, 126.60, -1.8 dB, respectively at H- plane.

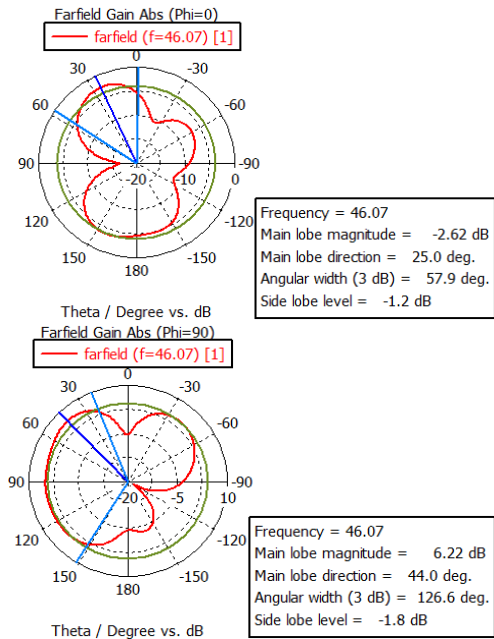


Fig. 6. E and H-plane radiation patterns for multiband millimetre antenna at  $f_{r1,2} = 46.07$  GHz.

Fig. 7 shows the radiation pattern of electric field and magnetic field at  $f_{r1,3} = 56.74$  GHz. At this frequency the

magnitude and direction of main lobe, half power beam width (3 dB) and side lobe magnitude are 2.83 dB and 30.00, 74.70, -7.1 dB, respectively at E- plane. Moreover, the magnitude and direction of main lobe, half power beam width (3 dB) and side lobe magnitude are 7.49 dB and 108.00, 91.90, -5.9 dB, respectively at H- plane.

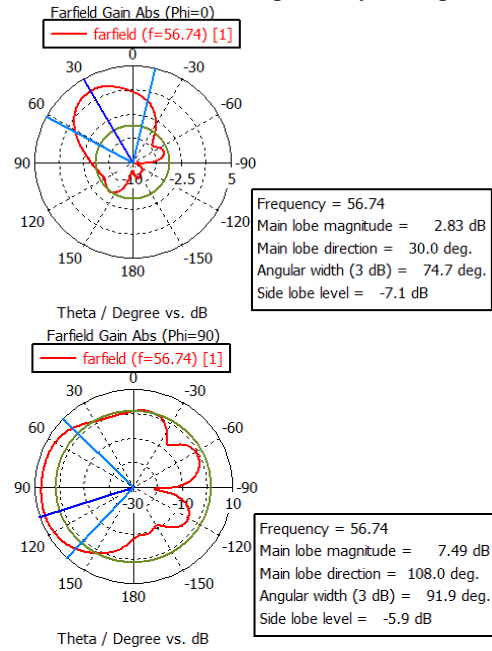


Fig. 7. E and H-plane radiation patterns for multiband millimetre antenna at  $f_{r1,3} = 56.74$  GHz.

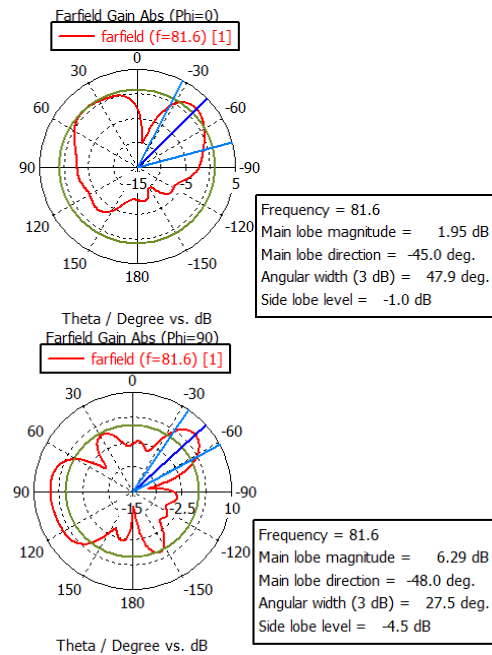


Fig. 8. E and H-plane radiation patterns for multiband millimetre antenna at  $f_{r1,4} = 81.6$  GHz.

Fig. 8 shows the radiation pattern of electric field and magnetic field at  $f_{r1,4} = 81.6$  GHz. At this frequency the magnitude and direction of main lobe, half power beam width (3 dB) and side lobe magnitude are 1.95 dB and -

45.00, 47.90, -1.0 dB respectively at E- plane. Moreover, the magnitude and direction of main lobe, half power beam width (3 dB) and side lobe magnitude are 6.29 dB, -48.00, 27.50, -4.5 dB, respectively at H- plane.

Fig. 9 shows the radiation pattern of the electric field and magnetic field at  $f_{r1,5} = 110.09$  GHz. At this frequency, the magnitude and direction of the main lobe, half power beam width (3dB) and side lobe magnitude are 3.17 dB and  $45.0^\circ$ ,  $41.5^\circ$ , -2.0 dB, respectively at E-plane. Moreover, at the magnitude and direction of the main lobe, half-power beam width (3 dB) and side lobe magnitude are 4.36 dB and  $-60.0^\circ$ ,  $39.0^\circ$ , -1.0 dB, respectively at H- plane.

3) Voltage Standing Wave Ratio (VSWR)

Simulation results of VSWR are also obtained and shown in Fig. 10. The values of VSWR at  $f_{r1,1}=35.84$  GHz,  $f_{r1,2}=46.07$  GHz,  $f_{r1,3} = 56.74$  GHz,  $f_{r1,4}=81.6$  GHz, and  $f_{r1,5}=110.09$  GHz are 1.0886, 1.4111, 1.3353, 1.1275 and 1.3816, respectively. Due to considerable impedance matching, the VSWR value is below 1.5.

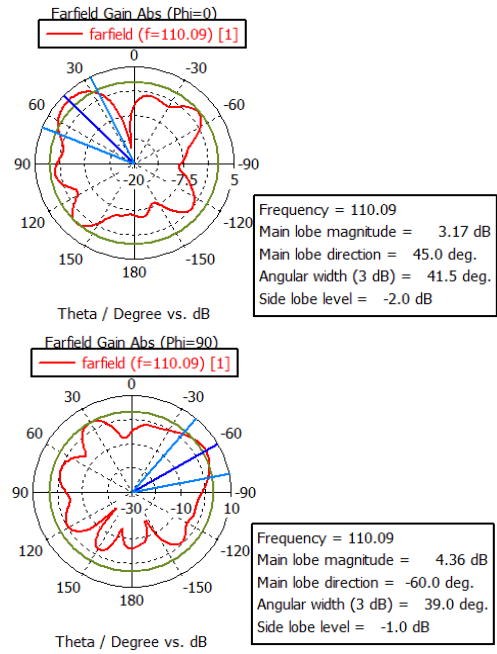


Fig. 9. E and H-plane radiation patterns for multiband millimetre antenna at  $f_{r1,5} = 110.09$  GHz.

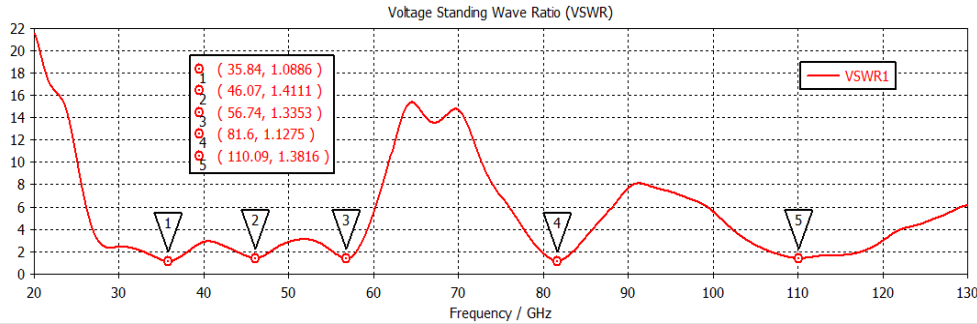


Fig. 10. VSWR curve of the multiband millimetre wave antenna.

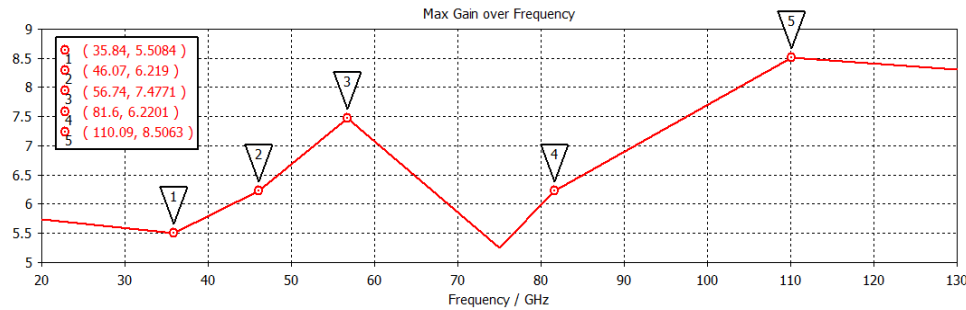


Fig. 11. Maximum Gain vs Frequency curve of the multiband millimetre wave antenna.

4) Gain and directivity

Fig. 11 shows gains at resonance frequencies  $f_{r1,1}=35.84$  GHz,  $f_{r1,2}=46.07$  GHz,  $f_{r1,3} = 56.74$  GHz,  $f_{r1,4}=81.6$  GHz, and  $f_{r1,5}=110.09$  GHz. The gain at  $f_{r1,1}$  is 5.5084 dB, at  $f_{r1,2}$  is 6.219 dB, at  $f_{r1,3}$  is 7.4771 dB, at  $f_{r1,4}$  is 6.2201 dB and at  $f_{r1,5}$  is 8.5063 dB and the directivity at  $f_{r1,1}$ ,  $f_{r1,2}$ ,  $f_{r1,3}$ ,  $f_{r1,4}$  and  $f_{r1,5}$ , are 6.686 dB, 6.640 dB, 7.793 dB, 6.486dB, and 8.797 dB, respectively.

5) Radiation efficiency

The ratio of antenna gain to directivity is simply called antenna efficiency and it is represented as  $\eta = G$  (dB)- $D$  (dB). The efficiency of the antenna are 76.26%, 90.76%, 92.98%, 94.06%, and 93.52% at  $f_{r1,1}$ ,  $f_{r1,2}$ ,  $f_{r1,3}$ ,  $f_{r1,4}$  and  $f_{r1,5}$ , respectively. The radiation Efficiency of the multiband millimetre wave antenna is presented in Fig. 12.

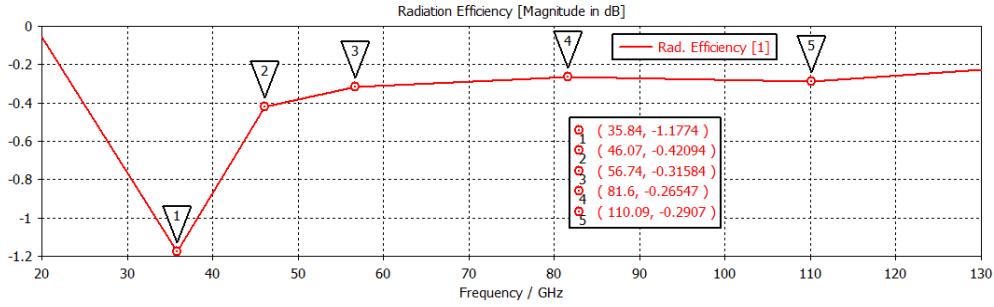


Fig. 12. Radiation Efficiency curve of the multiband millimetre wave antenna.

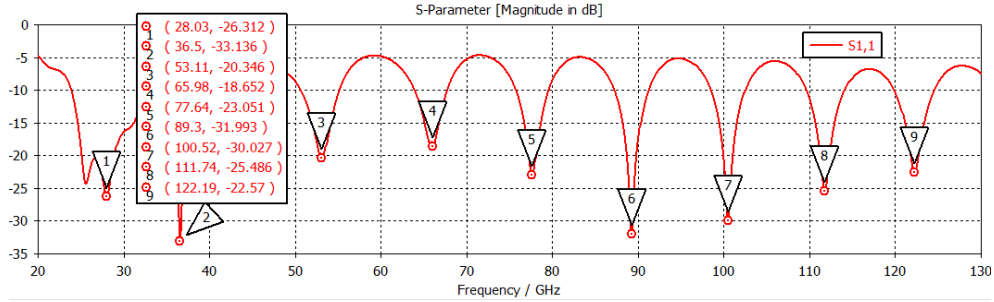


Fig. 13. Reflection co-efficient (S11) of the multiband millimetre wave array antenna.

**B. Simulation Results of the Array Antenna**

The optimized results of the designed antenna using waveguide ports are at resonance frequencies at  $f_{r2,1}$  =28.03 GHz,  $f_{r2,2}$  =36.5 GHz,  $f_{r2,3}$  = 53.11 GHz,  $f_{r2,4}$  =65.98 GHz,  $f_{r2,5}$  =77.64 GHz,  $f_{r2,6}$  =89.3 GHz,  $f_{r2,7}$  = 100.52 GHz,  $f_{r2,8}$  =111.74 GHz and  $f_{r2,9}$  =122.19 GHz are presented in this section.

**1) Return loss (s-parameter) and bandwidth**

The simulated return loss at  $f_{r2,1}$  is 26.213 dB, at  $f_{r2,2}$  is 33.136 dB, at  $f_{r2,3}$  is 20.345 dB, at  $f_{r2,4}$  is 18.651 dB, at  $f_{r2,5}$  is 23.05 dB, at  $f_{r2,6}$  is 31.99 dB, at  $f_{r2,7}$  is 30.027 dB, at  $f_{r2,8}$  is 25.486 dB and at  $f_{r2,9}$  is 22.569 dB, which are shown in Fig. 13. In this antenna also all the return losses are more than 10 dB which indicates antenna impedance and the waveguide port impedance is considerably matched. For this less amount of power is reflected back from the input port of the antenna. Fig. 13 also shows impedance BW at these nine resonances are 8.91 GHz with a span from 23.85 GHz to 32.76 GHz, 8.14 GHz with a span from 34.74 GHz to 42.88 GHz, 4.4 GHz with a span from 50.69 GHz to 55.09 GHz, 3.63 GHz with a span from 64.00 GHz to 67.63 GHz, and 3.73 GHz with a span from 75.77 GHz to 79.5 GHz, 3.85 GHz with a span from 87.32 GHz to 91.17 GHz, 3.85 GHz with a span from 98.54 GHz to 102.39 GHz, 4.4 GHz with a span from 109.65 GHz to 114.05 GHz, and 4.51 GHz with a span from 119.99 GHz to 124.5 GHz, respectively. The %BW of the array antenna are 31.78%, 22.3%, 8.28%, 5.5%, 4.8%, 4.31%, 3.83%, 3.93%, and 3.69% at  $f_{r2,1}$ ,  $f_{r2,2}$ ,  $f_{r2,3}$ ,  $f_{r2,4}$ ,  $f_{r2,5}$ ,  $f_{r2,6}$ ,  $f_{r2,7}$ ,  $f_{r2,8}$ , and  $f_{r2,9}$  respectively

**2) Radiation pattern**

Fig. 14 to Fig. 22 shows far field E and H-field patterns at  $f_{r2,1}$ ,  $f_{r2,2}$ ,  $f_{r2,3}$ ,  $f_{r2,4}$ ,  $f_{r2,5}$ ,  $f_{r2,6}$ ,  $f_{r2,7}$ ,  $f_{r2,8}$ , and  $f_{r2,9}$ , respectively indicating the magnitude of the main lobe, half power beam width (3 dB) and side lobe magnitude.

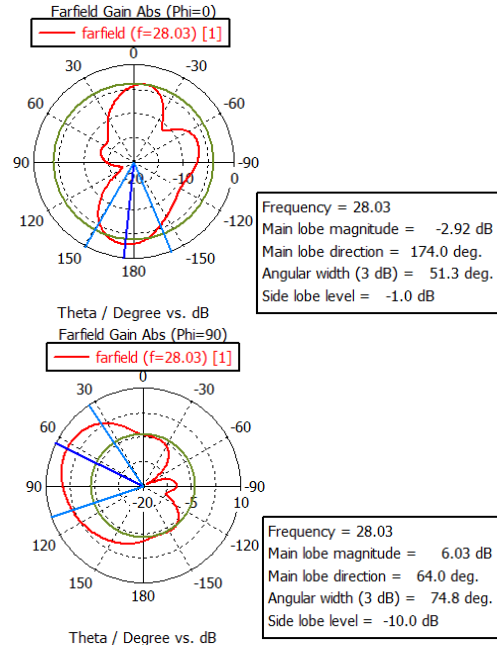


Fig. 14. E and H-plane radiation patterns for multiband millimetre array antenna at  $f_{r2,1}$  = 28.03 GHz.

Fig. 14 shows the radiation pattern of the electric field and magnetic field at  $f_{r2,1}$  = 28.03 GHz. At this frequency, the magnitude and direction of the main lobe, half power beam width (3 dB), and side lobe magnitude are -2.92 dB and 174.00, 51.30, -1.0 dB, respectively at E- plane.

Moreover, at the magnitude and direction of the main lobe, half power beam width (3 dB) and side lobe magnitude are 6.03 dB, and 64.00, 74.80, -10.0 dB, respectively at H-plane.

Fig. 15 shows the radiation pattern of the electric field and magnetic field at  $f_{r,2,2}=36.5$  GHz. At this frequency, the magnitude and direction of the main lobe, half power beam width (3 dB) and side lobe magnitude are -1.37 dB and 180.0°, 35.8°, -4.1 dB, respectively at E- plane. Moreover, the magnitude and direction of the main lobe, half power beam width (3 dB) and side lobe magnitude are 7.6 dB and 70.0°, 68.5°, -10.6 dB, respectively at H- plane.

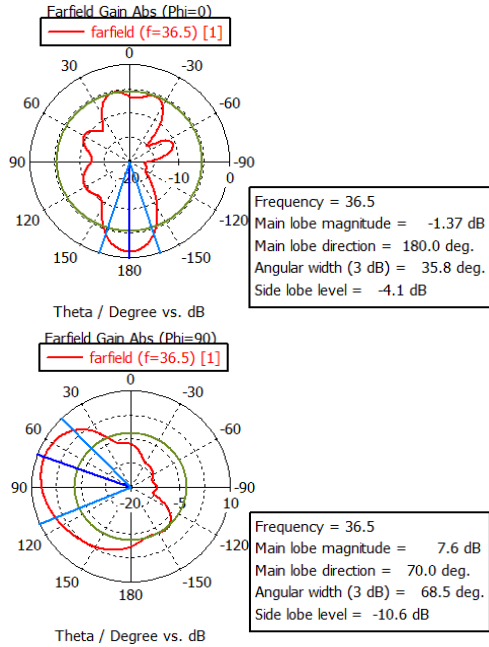


Fig. 15. E and H-plane radiation patterns for multiband millimetre antenna at  $f_{r,2,2} = 36.5$  GHz.

Fig. 16 shows the radiation pattern of the electric field and magnetic field at  $f_{r,2,3} = 53.11$  GHz. At this frequency, the magnitude and direction of the main lobe, half power beam width (3 dB) and side lobe magnitude are 6.8 dB and 0.0°, 26.6°, -4.0 dB, respectively at E- plane. Moreover, the magnitude and direction of the main lobe, half power beam width (3 dB) and side lobe magnitude are 9.12 dB and 78.0°, 82.9°, -2.3 dB respectively at H- plane.

Fig. 17 shows the radiation pattern of the electric field and magnetic field at  $f_{r,2,4} = 65.98$  GHz. At this frequency, the magnitude and direction of the main lobe, half power beam width (3 dB) and side lobe magnitude are 3.35 dB and 0.0°, 23.3°, -1.4 dB, respectively at E- plane. Moreover, the magnitude and direction of the main lobe, half power beam width (3 dB) and side lobe magnitude are 10.2 dB, 85.0°, 89.0°, -5.3 dB, respectively at H- plane.

Fig. 18 shows the radiation pattern of the electric field and magnetic field at  $f_{r,2,5} = 77.64$  GHz. At this frequency, the magnitude and direction of the main lobe, half power beam width (3 dB) and side lobe magnitude are 3.49 dB and 180.0°, 18.2°, -1.3 dB respectively at E- plane. Moreover, the magnitude and direction of the main lobe, half power beam width (3 dB) and side lobe magnitude are 10.7 dB and 72.0°, 79.4°, -7.6 dB, respectively at H- plane.

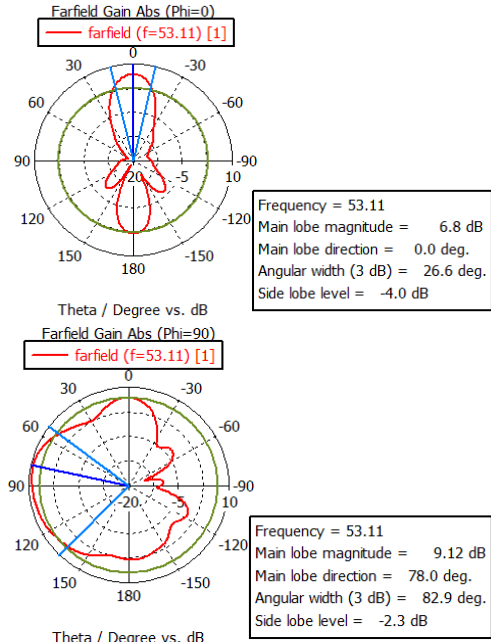


Fig. 16. E and H-plane radiation patterns for multiband millimetre antenna at  $f_{r,2,3} = 53.11$  GHz.

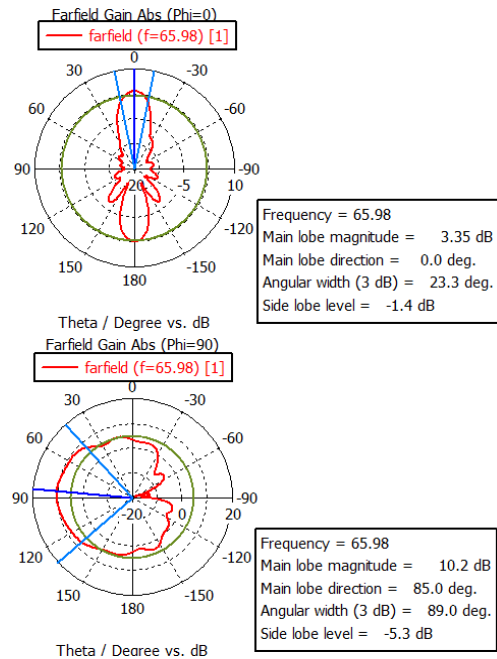


Fig. 17. E and H-plane radiation patterns for multiband millimetre antenna at  $f_{r,2,4} = 65.98$  GHz.

Fig. 19 shows the radiation pattern of the electric field and magnetic field at  $f_{r,2,6} = 89.3$  GHz. At this frequency, the magnitude and direction of the main lobe, half power beam width (3 dB), and side lobe magnitude are 3.73 dB and  $180.0^\circ$ ,  $18.4^\circ$ ,  $-3.8$  dB respectively at the E- plane. Moreover, the magnitude and direction of the main lobe, half power beam width (3 dB), and side lobe magnitude are 12.1 dB and  $95.0^\circ$ ,  $62.5^\circ$ ,  $-1.9$  dB, respectively at H- plane.

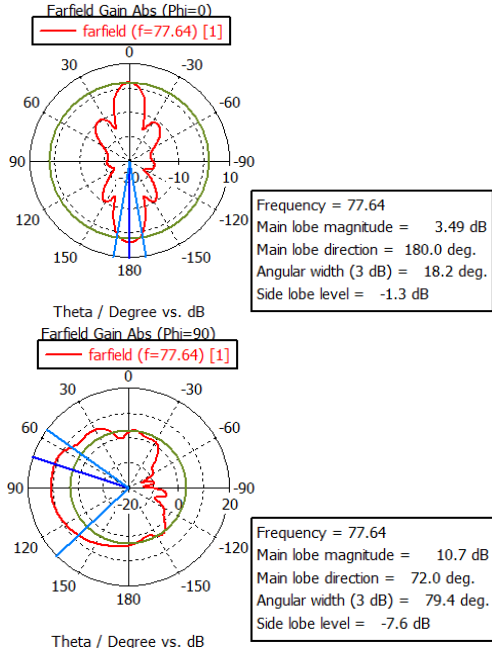


Fig. 18. E and H-plane radiation patterns for multiband millimetre antenna at  $f_{r,2,5} = 77.64$  GHz.

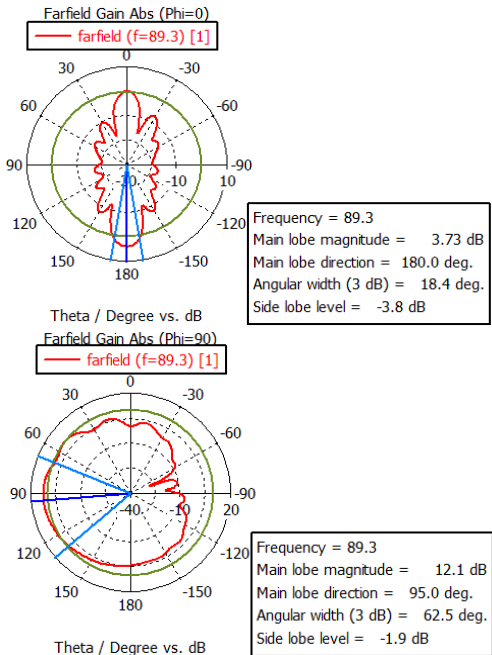


Fig. 19. E and H-plane radiation patterns for multiband millimetre antenna at  $f_{r,2,6} = 89.3$  GHz.

Fig. 20 shows the radiation pattern of the electric field and magnetic field at  $f_{r,2,7} = 100.52$  GHz. At this frequency, the magnitude and direction of the main lobe, half power beam width (3 dB), and side lobe magnitude are 4.69 dB and  $180.0^\circ$ ,  $15.3^\circ$ ,  $-12.1$  dB, respectively at E- plane. Moreover, the magnitude and direction of the main lobe, half power beam width (3 dB), and side lobe magnitude are 12.2 dB and  $31.0^\circ$ ,  $17.3^\circ$ ,  $-1.0$  dB, respectively at H- plane.

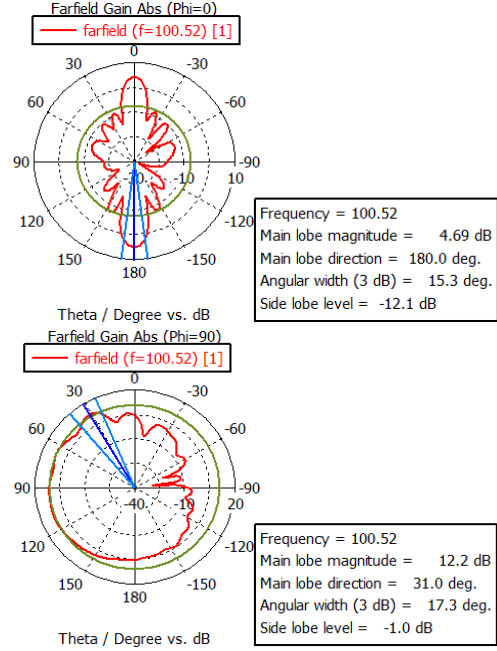


Fig. 20. E and H-plane radiation patterns for multiband millimetre antenna at  $f_{r,2,7} = 100.52$  GHz.

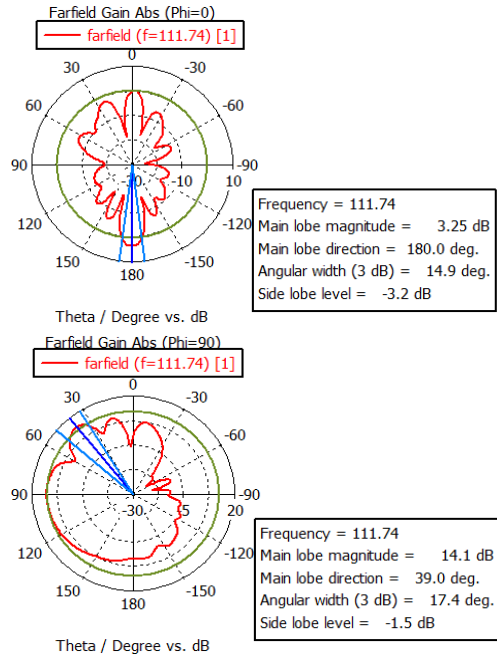


Fig. 21. E and H-plane radiation patterns for multiband millimetre antenna at  $f_{r,2,8} = 111.74$  GHz.

Fig. 21 shows the radiation pattern of the electric field and magnetic field at  $f_{r,2,8} = 111.74$  GHz. At this frequency, the magnitude and direction of the main lobe, half power beam width (3 dB) and side lobe magnitude are 3.25 dB,  $180.0^{\circ}$ ,  $14.9^{\circ}$ , -3.2 dB, respectively at E-plane. Moreover, the magnitude and direction of the main lobe, half power beam width (3 dB) and side lobe magnitude are 14.1 dB,  $39.0^{\circ}$ ,  $17.4^{\circ}$ , -1.5 dB, respectively at H-plane.

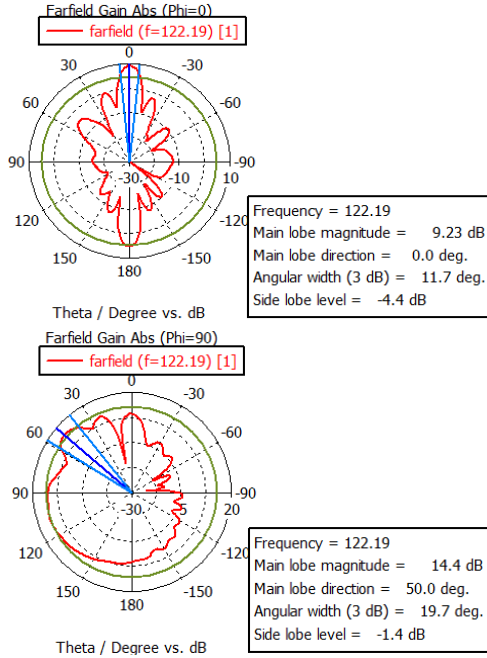


Fig. 22. E and H-plane radiation patterns for multiband millimetre antenna at  $f_{r,2,9} = 122.19$  GHz.

Fig. 22 shows the radiation pattern of the electric field and magnetic field at  $f_{r,2,9} = 122.19$  GHz. At this

frequency, the magnitude and direction of the main lobe, half power beam width (3 dB) and side lobe magnitude are 9.23 dB,  $0.0^{\circ}$ ,  $11.7^{\circ}$ , -4.4 dB, respectively at E-plane. Moreover, the magnitude and direction of the main lobe, half power beam width (3 dB) and side lobe magnitude are 14.4 dB,  $50.0^{\circ}$ ,  $19.7^{\circ}$ , -1.4 dB, respectively at H-plane.

3) Voltage standing wave ratio (VSWR)

Simulation results of VSWR are also obtained and shown in Fig. 23. The values of VSWR at  $f_{r,2,1} = 28.03$  GHz,  $f_{r,2,2} = 36.5$  GHz,  $f_{r,2,3} = 53.11$  GHz,  $f_{r,2,4} = 65.98$  GHz,  $f_{r,2,5} = 77.64$  GHz,  $f_{r,2,6} = 89.3$  GHz,  $f_{r,2,7} = 100.52$  GHz,  $f_{r,2,8} = 111.74$  GHz and  $f_{r,2,9} = 122.19$  GHz are 1.1016, 1.0451, 1.2126, 1.2645, 1.1514, 1.0516, 1.0651, 1.1123 and 1.1607, respectively. Due to considerable impedance matching, the VSWR value is below 1.5.

4) Gain and directivity

Fig. 24 shows gains at resonance frequencies  $f_{r,2,1} = 28.03$  GHz,  $f_{r,2,2} = 36.5$  GHz,  $f_{r,2,3} = 53.11$  GHz,  $f_{r,2,4} = 65.98$  GHz,  $f_{r,2,5} = 77.64$  GHz,  $f_{r,2,6} = 89.3$  GHz,  $f_{r,2,7} = 100.52$  GHz,  $f_{r,2,8} = 111.74$  GHz and  $f_{r,2,9} = 122.19$  GHz. The gain at  $f_{r,2,1}$  is 6.0259 dB, at  $f_{r,2,2}$  is 7.5952 dB, at  $f_{r,2,3}$  is 9.1017 dB, at  $f_{r,2,4}$  is 10.234 dB, at  $f_{r,2,5}$  is 10.669 dB, at  $f_{r,2,6}$  is 12.063 dB, at  $f_{r,2,7}$  is 12.117 dB, at  $f_{r,2,8}$  is 14.073 dB, and at  $f_{r,2,9}$  is 14.395 dB and the directivity at  $f_{r,2,1}$ ,  $f_{r,2,2}$ ,  $f_{r,2,3}$ ,  $f_{r,2,4}$ ,  $f_{r,2,5}$ ,  $f_{r,2,6}$ ,  $f_{r,2,7}$ ,  $f_{r,2,8}$ , and  $f_{r,2,9}$  are 9.144 dB, 10.57 dB, 10.57 dB, 11.85 dB, 12.35 dB, 13.72 dB, 13.62 dB, 15.31 dB and 15.58 dB, respectively.

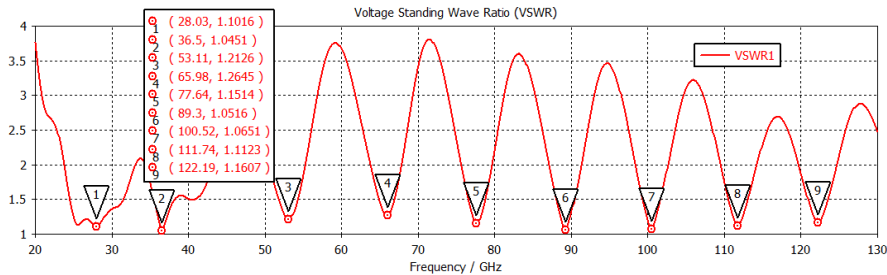


Fig. 23. VSWR curve of the multiband millimetre wave array antenna.

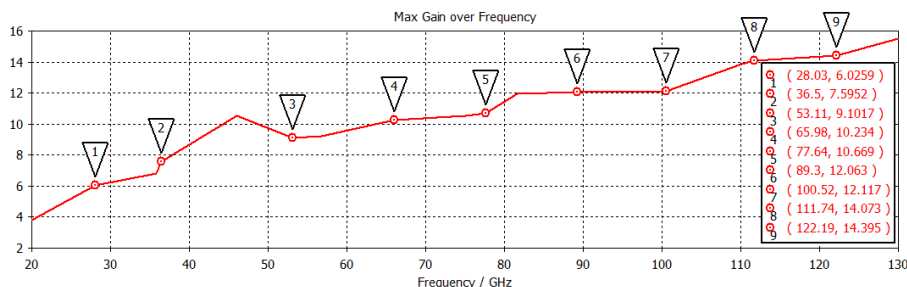


Fig. 24. Maximum gain vs frequency curve of the multiband millimetre wave array antenna.

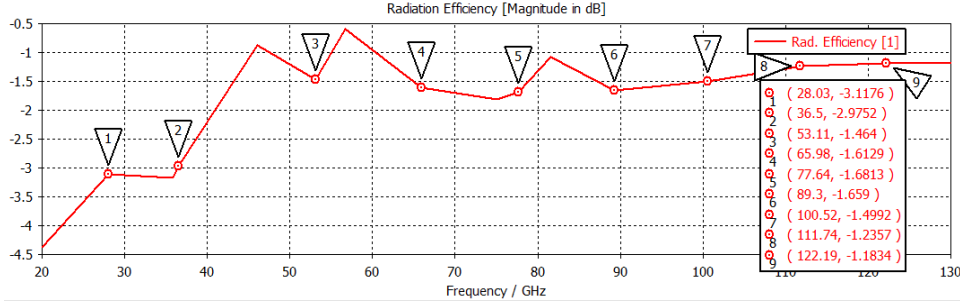


Fig. 25. Radiation efficiency curve of the multiband millimetre wave array antenna.

5) Radiation efficiency

The ratio of antenna gain to directivity is simply called antenna efficiency and it is represented as  $\eta = G \text{ (dB)} - D \text{ (dB)}$ . The efficiency are 48.77 %, 50.40%, 71.38%, 68.97%, 67.9%, 68.25%, 70.81%, 75.23%, and 76.15% at frequencies  $f_{r2,1}$ ,  $f_{r2,2}$ ,  $f_{r2,3}$ ,  $f_{r2,4}$ ,  $f_{r2,5}$ ,  $f_{r2,6}$ ,  $f_{r2,7}$ ,  $f_{r2,8}$ , and  $f_{r2,9}$ , respectively. The radiation Efficiency of the multiband millimetre wave antenna is shown in Fig. 25.

The complete summary of simulation results of the two designed antennas is mentioned in Table III.

IV. COMPARATIVE STUDY OF ANTENNAS

In this section, the proposed antennas are compared with the antennas described in the relevant literature. Though both of the proposed antennas have several resonance frequencies as targeted to design the antenna at a higher frequency, only the frequencies in the W band and D band are mentioned. The comparison is done in terms of the total size of the antenna, operating frequency,

bandwidth, and gain which is given in Table IV. The proposed single antenna is smaller in size than all the existing antennas considered in the literature review, except the one reported in [7] which has only one frequency in the W and D bands whereas the proposed antenna has two. The antennas reported in [3] and [16] have multiple frequencies; however, none of them are as high as the proposed single antenna having 110 GHz. Some studies [7] and [23] reported antennas with frequencies of 122 GHz and 146 GHz respectively. However, the gain and bandwidth in antenna [7] are not mentioned and the antenna reported in [23] is almost four times the size of the proposed single antenna. Hence, our proposed single antenna is best suited for practical applications. The array antenna is proposed for the high gain and directivity requirements. It has five operating frequencies in the W and D band regions, with the highest frequency at 122 GHz. From Table IV, it is clear that the proposed array antenna has high gains in almost five operating frequencies.

TABLE III: RESULTS OF THE ANTENNAS

Antenna	Size (mm <sup>2</sup> )	Resonant Frequency (GHz)	S-parameters (dB)	VSWR	Gain (dB)	Directivity (dB)	-10 dB Bandwidth (GHz)	Rad. efficiency (%)
Single Antenna	4.8 x 5.4	$f_{r1,1} = 35.84$	-27.45	1.088	5.508	6.686	4.84	76.26
		$f_{r1,2} = 46.07$	-15.365	1.411	6.219	6.64	3.63	90.76
		$f_{r1,3} = 56.74$	-16.858	1.335	7.477	7.793	2.42	92.98
		$f_{r1,4} = 81.6$	-24.447	1.127	6.22	6.486	3.3	94.06
		$f_{r1,5} = 110.09$	-15.904	1.38	8.506	8.797	10.01	93.52
Array Antenna	11.1 x 6.4	$f_{r2,1} = 28.03$	-26.213	1.101	6.026	9.144	8.91	48.77
		$f_{r2,2} = 36.5$	-33.136	1.045	7.595	10.57	8.14	50.4
		$f_{r2,3} = 53.11$	-20.345	1.212	9.102	10.57	4.4	71.38
		$f_{r2,4} = 65.98$	-18.651	1.264	10.23	11.85	3.63	68.97
		$f_{r2,5} = 77.64$	-23.05	1.151	10.67	12.35	3.73	67.9
		$f_{r2,6} = 89.3$	-31.99	1.051	12.06	13.72	3.85	68.25
		$f_{r2,7} = 100.52$	-30.027	1.065	12.12	13.62	3.85	70.81
		$f_{r2,8} = 111.74$	-25.486	1.112	14.07	15.31	4.4	75.23
		$f_{r2,9} = 122.19$	-22.569	1.16	14.39	15.58	4.51	76.15

TABLE IV: COMPARISON OF THE SIMULATED ANTENNA RESULTS WITH THE LITERATURE

Reference Antennas	Size (mm <sup>2</sup> )	Operating Bands (GHz)	% Bandwidth	Gain (dB)
Ref [3]	40×40	85, 94	8.53, 1.81	8.28, 8.89
Ref [4]	9×3	94	7.44	23
Ref [19]	14.44×4.46	86,97,104	-	>10
Ref [20]	13×34.99	94	36.49	16.7
Ref [7]	7×3.5	122	-	-
Ref [26]	10×10	146	14.38	14.5
Proposed Single Antenna	4.8 × 5.4	81.6, 110.09	4.04, 9.09	6.22, 8.5
Proposed Array Antenna	11.1 × 6.4	77.64, 89.3, 100.52, 111.74, 122.19	4.8, 4.31, 3.83, 3.93, 3.69	10.67, 12.06, 12.12, 14.07, 14.39

## V. CONCLUSION

Two multiband antennas with resonance frequencies in the millimetre band are proposed in this paper. The first antenna with a small size of 4.8 mm by 5.4 mm has five operating frequencies at frequencies 35.84 GHz, 46.07 GHz, 56.74 GHz, 81.6 GHz and 110.09 GHz. The s-parameter (S<sub>11</sub>), bandwidth, VSWR, antenna gain, directivity, and radiation efficiency at five resonance frequencies are (-27.45 dB, 4.84 GHz, 1.0886, 5.508 dB, 6.686 dBi, and 76.26%), (-15.365 dB, 3.63 GHz, 1.4111, 6.219 dB, 6.64 dBi, and 90.76%), (-16.858 dB, 2.42 GHz, 1.335, 7.477 dB, 7.793 dBi, and 92.98%), (-24.447 dB, 3.3 GHz, 1.1275, 6.22 dB, 6.486 dBi, and 94.06%), and (-15.904 dB, 10.01 GHz, 1.3816, 8.506 dB, 8.797 dBi, and 93.52%), respectively. The second antenna is an array antenna with nine resonance frequencies which is made from the first antenna. The dimension of the antenna is 11.1 mm by 6.4 mm which is larger than the single antenna. The highest five resonance frequencies of the second antenna are in the W and D bands which are 77.64GHz, 89.3 GHz, 100.52 GHz, 111.74 GHz, and 122.19 GHz. The s-parameter (S<sub>11</sub>), bandwidth, VSWR, antenna gain, directivity, and radiation efficiency) at those five resonance frequencies are (-23.05 dB, 3.73 GHz, 1.1514, 10.68 dB, 12.35 dBi, and 67.9%), (-31.99 dB, 3.85 GHz, 1.0516, 12.06 dB, 13.72 dBi, and 68.25%), (-30.027 dB, 3.85 GHz, 1.0651, 12.12 dB, 13.62 dBi, and 70.81%), (-25.486 dB, 4.4 GHz, 1.1123, 14.07 dB, 15.31 dBi, and 75.23%), and (-22.569 dB, 4.51 GHz, 1.1607, 14.39 dB, 15.58 dBi, and 76.15%), respectively.

Although the single antenna provides higher radiation efficiency than the array antenna, the array antenna is superior in terms of BW, gain and directivity. When antenna size is important, the single antenna can be used. For higher gain and directivity, the array antenna can be used though it has a slightly larger size than a single antenna. However, in comparison with the previous work reported in the literature, the array antenna is still compact in size. These two proposed antennas can be used in multiple applications, including the internet of

things, imaging technology, biomedical applications, and interferometry radars.

## CONFLICT OF INTEREST

The authors declare no conflict of interest.

## AUTHOR CONTRIBUTIONS

Conceptualization: Abdullah Khan Galib, Nayan Sarker, M. Rubaiyat Hossain Mondal; Methodology: Abdullah Khan Galib, Nayan Sarker; Formal analysis and investigation: Abdullah Khan Galib, Nayan Sarker; Writing—original draft preparation: Abdullah Khan Galib, Nayan Sarker; Writing—review and editing: M. Rubaiyat Hossain Mondal; Supervision: M. Rubaiyat Hossain Mondal. All authors had approved the final version.

## REFERENCES

- [1] S. Agarwal, N. P. Pathak, and D. Singh, "Performance comparison of microstrip patch antenna for 94 GHz imaging applications," in *Proc. 7th International Conference on Industrial and Information Systems (ICIIS)*, Chennai, India, 2012, pp. 1-4.
- [2] P. Rodriguez-Vazquez, J. Grzyb, B. Heinemann, and U. R. Pfeiffer, "A QPSK 110-Gb/s polarization-diversity MIMO wireless link with a 220–255 GHz tunable LO in a SiGe HBT technology," *IEEE Transactions on Microwave Theory and Techniques*, vol. 68, no. 9, pp. 3834-3851, Sept. 2020.
- [3] S. Agarwal, N. P. Pathak, and D. Singh, "Concurrent 85GHz/94GHz slotted gap coupled parasitic microstrip antenna for millimeter wave applications," in *Proc. National Conference on Communications (NCC)*, New Delhi, India, 2013, pp. 1-5.
- [4] C. Zech, A. Hülsmann, M. Schlechtweg, L. Georgi, H. Gulan, and O. Ambacher, "A compact, universal and cost-efficient antenna setup for mmW-radar applications," in *Proc. International Conference on Radar*, Adelaide, Australia, 2013, pp. 417-421.
- [5] W. Ahmad, M. Kucharski, H. Ng, and D. Kissinger, "A compact efficient D-Band micromachined On-Chip differential patch antenna for radar applications\*," in *Proc. International Symposium on Antennas and Propagation*

- and USNC-URSI Radio Science Meeting, Atlanta, USA, 2019, pp. 2201-2202.
- [6] Z. Shen, N. Ito, E. Sakata, C. W. Domier, N. C. Luhmann, and A. Mase, "D-band double dipole antenna for use in millimeter wave imaging systems," in *Proc. IEEE Antennas and Propagation Society International Symposium*, Honolulu, USA, 2007, pp. 2658-2661.
- [7] A. Bhutani, B. Goettel, M. Pauli, and T. Zwick, "122 GHz FMCW radar system-in-package in LTCC technology," in *Proc. 49th European Microwave Conference (EuMC)*, Paris, France, 2019, pp. 1008-1011.
- [8] T. Chaloun, P. Hügler, and C. Waldschmidt, "A wideband 122GHz cavity-backed dipole antenna for millimeter-wave radar altimetry," in *Proc. 14th European Conference on Antennas and Propagation (EuCAP)*, Copenhagen, Denmark, 2020, pp. 1-4.
- [9] A. Mir and J. Yu, "Broadband circular polarized cross bow tie antenna for terahertz range," in *Proc. IEEE Antennas and Propagation Society International Symposium*, Memphis, USA, 2014, pp. 416-417.
- [10] S. Ullah, C. Ruan, and T. U. Haq, "Z-Shaped dual band circular polarized microstrip antenna for THz communication," in *Proc. 44th International Conference on Infrared, Millimeter, and Terahertz Waves*, Paris, France, 2019, pp. 1-2.
- [11] E. Chemweno, P. Kumar, and A. Thomas, "Substrate integrated waveguide-dielectric resonator antenna for future wireless communication," *SAIEE Africa Research Journal*, vol. 113, no. 3, pp. 119-128.
- [12] H. Kim, W. Choe, and J. Jeong, "A terahertz CMOS V-Shaped patch antenna with defected ground structure," *Sensors*, vol. 18, no. 8, p. 2432, 2018.
- [13] K. A. Kuznetsov, D. A. Safronkov, P. I. Kuznetsov, and G. K. Kitaeva, "Terahertz photoconductive antenna based on a topological insulator nanofilm," *Applied Sciences*, vol. 11, no. 12, p. 5580, 2021.
- [14] S. Agarwal, N. P. Pathak, and D. Singh, "Concurrent 83GHz/94 GHz parasitically coupled defected microstrip feedline antenna for millimeter wave applications," in *Proc. Applied Electromagnetics Conferenc*, Bhubaneswar, India, 2013, pp. 1-2.
- [15] N. Vannod, C. Algani, F. Deshours, and G. Alquie, "Study and integration of a wideband antenna working in the millimeter-wave band (D-band)," in *Proc. European Conference on Wireless Technologies*, Munich, Germany, 2007, pp. 51-54.
- [16] A. K. Galib, N. Sarker, and M. R. H. Mondal, "Two compact multiband millimetre wave antennas for wireless communication," in *Proc. International Conference on Telecommunications and Photonics*, Dhaka, Bangladesh, 2019, pp. 1-4.
- [17] X. Li, J. Xiao, and J. Yu, "Long-Distance wireless mm-wave signal delivery at W-Band," *Journal of Lightwave Technology*, vol. 34, no. 2, pp. 661-668, 15 Jan. 2016.
- [18] Q. Wang, Z. H. Shao, Y. J. Cheng, and P. K. Li, "Ka/W dual-band reflectarray antenna for dual linear polarization," *IEEE Antennas and Wireless Propagation Letters*, vol. 16, pp. 1301-1304, 2017.
- [19] A. Mirbeik-Sabzevari, S. Li, E. Garay, H. Nguyen, H. Wang, and N. Tavassolian, "W-Band micromachined antipodal vivaldi antenna using SIW and CPW structures," *IEEE Transactions on Antennas and Propagation*, vol. 66, no. 11, pp. 6352-6357, Nov. 2018.
- [20] N. Wang, B. Zhao, M. Fang, J. Qiu, and L. Xiao, "An ultra-wideband fermi tapered slot antenna with waveguide-microstrip transition device," in *Proc. IEEE International Symposium on Antennas and Propagation & USNC/URSI National Radio Science Meeting*, Boston, MA, USA, 2018, pp. 609-610.
- [21] N. Sarker, M. A. Islam, and M. R. H. Mondal, "Two novel multiband centimetre-wave patch antennas for a novel OFDM based RFID system," *Journal of Communications*, vol. 13, no. 6, 2018.
- [22] N. Sarker and M. R. H. Mondal, "Design and analysis of double E-shaped array antennas for an outdoor RFID system," in *Proc. IEEE International Conference on Electrical and Computer Engineering*, Dhaka, Bangladesh, 2018, pp. 1-4.
- [23] Y. Dong, T. K. Johansen, V. Zhurbenko, and P. J. Hanberg, "A rectangular waveguide-to-coplanar waveguide transition at D-band using wideband patch antenna," in *Proc. 48th European Microwave Conference (EuMC)*, Madrid, Spain, 2018, pp. 1045-1048.
- [24] L. Marnat, K. Medrar, and L. Dussopt, "Highly integrable high gain substrate-integrated planar lens for wide D-band applications," in *Proc. 14th European Conference on Antennas and Propagation (EuCAP)*, Copenhagen, Denmark, 2020, pp. 1-4.
- [25] A. Lamminen, J. Säily, J. Ala-Laurinaho, J. de Cos, and V. Ermolov, "Patch antenna and antenna array on multilayer high-frequency PCB for D-Band," *IEEE Open Journal of Antennas and Propagation*, vol. 1, pp. 396-403, 2020.
- [26] B. Zhang, C. Kärfelt, H. Gulan, T. Zwick, and H. Zirath, "A D-Band packaged antenna on organic substrate with high fault tolerance for mass production," *IEEE Transactions on Components, Packaging and Manufacturing Technology*, vol. 6, no. 3, pp. 359-365, March 2016.
- [27] D. Hou, Y. Xiong, W. Goh, S. Hu, W. Hong, and M. Madihian, "130-GHz On-Chip meander slot antennas with stacked dielectric resonators in standard CMOS technology," *IEEE Transactions on Antennas and Propagation*, vol. 60, no. 9, pp. 4102-4109, Sept. 2012.
- [28] K. Anim, J. N. Lee, and Y. B. Jung, "High-Gain millimeter-wave patch array antenna for unmanned aerial vehicle application," *Sensors*, vol. 21, no. 11, pp. 3914, 2021.
- [29] P. Kumar, "Antennas and arrays for 60 GHz high data rate wireless applications," *International Journal on Communications Antenna and Propagation*, vol. 9, no. 4, pp. 255-262, 2019.
- [30] J. Khan, S. Ullah, U. Ali, F. A. Tahir, I. Peter, and L. Matekovits, "Design of a millimeter-wave MIMO antenna array for 5G communication terminals," *Sensors*, vol. 22, no. 7, pp. 2768, 2022.

- [31] M. Mlungisi and P. Kumar, "A microstrip patch antenna with defected ground structure for triple band wireless communications," *Journal of Communications*, vol. 14, no. 8, pp. 684-688, 2019.

Copyright © 2023 by the authors. This is an open access article distributed under the Creative Commons Attribution License ([CC BY-NC-ND 4.0](https://creativecommons.org/licenses/by-nc-nd/4.0/)), which permits use, distribution and reproduction in any medium, provided that the article is properly cited, the use is non-commercial and no modifications or adaptations are made.



**Abdullah Khan Galib** received the B.Sc in electrical and electronic engineering (EEE) degree from University of Asia Pacific (UAP), Dhaka, Bangladesh in June, 2014 and the M. Engg degree in Information and Communication Technology (ICT) degree from Bangladesh University of Engineering and Technology (BUET), Dhaka, Bangladesh in July, 2021. He is also working as Senior System Engineer at a Telecommunication company, Dhaka, Bangladesh. His research interest is antenna design for 5G, RFID, IOT and OFDM.



**Nayan Sarker** received the B.Sc. in electronics and communication engineering (ECE) degree from Khulna University of Engineering and Technology (KUET), Khulna, Bangladesh in October, 2014. He received M.Sc. engineering degree at the Institute of Information and

Communication Technology (IICT) from Bangladesh University of Engineering and Technology (BUET), Dhaka, Bangladesh. He is also working as a lecturer at the dept. of electrical and electronic engineering (EEE), in Jatiya Kabi Kazi Nazrul Islam University, Mymensingh, Bangladesh. His research interest includes antenna design, OFDM, signal security and machine learning.



**M. Rubaiyat Hossain Mondal** received the B.Sc. and M.Sc. degrees in electrical and electronic engineering from Bangladesh University of Engineering and Technology (BUET), Dhaka, Bangladesh. He obtained the Ph.D. degree in 2014 from the Department of Electrical and Computer Systems Engineering, Monash University, Melbourne, Australia. From 2005 to 2010, and from 2014 to date he has been working as a Faculty Member at the Institute of Information and Communication Technology (IICT) in BUET. His research interests include wireless communications, optical wireless communications, OFDM, image processing and machine learning.